THE GUTS OF SOIL-STRUCTURE INTERACTION

John P WOLF[1] And Chongmin SONG[2]

SUMMARY

Salient features of soil-structure interaction are discussed. A criterion for the presence of radiation damping in a site is formulated. The radiation condition at infinity of outwardly propagating energy can for certain dynamic systems correspond to incoming waves. The consequences that the dynamic behaviour of the unbounded soil depends on the dimensionless frequency, which is proportional to the product of the frequency and the radial coordinate, are discussed. In addition, procedures to analyse the dynamic soil-structure interaction are outlined, ranging from the approximate simple physical models (cones, spring-dashpot-mass representations) for the soil to the damping-solvent extraction method and to the rigorous scaled boundary finite-element method. Convolution integrals can be avoided by constructing a dynamic system with a finite number of degrees of freedom for the soil. Extensions for moving concentrated loads and an increase in efficiency using a reduced set of functions are presented. The damping ratio of an equivalent one-degree-of-freedom system representing the interaction of the structure with the soil for a horizontal earthquake reflects the effect of the cutoff frequency for a soil layer.

Salient features and analysis methods of dynamic soil-structure interaction are outlined together with potential extensions. The selected topics are strongly influenced by the experience and personal preference of the authors. Only concepts and results are stated. For details, the reader should consult the references.

INTRODUCTION

In a dynamic soil-structure-interaction analysis a bounded structure (which can be nonlinear), consisting of the actual structure and an adjacent irregular soil if present, will interact with the unbounded (infinite or semi-infinite) soil assumed to be linear (Figure 1). The most striking feature in an unbounded soil, which is never encountered in a bounded medium is, in general, the *radiation of energy* towards infinity, leading to so-called *radiation damping* even in such a linear system. Mathematically, in a frequency-domain analysis, the dynamic stiffness relating the amplitudes of the displacements to those of the interaction forces in the nodes of the structure-soil interface of the unbounded soil is complex for all frequencies. As is well known, this occurs when the unbounded soil consists of a homogeneous half-space. But what happens to radiation damping for more general sites, e.g. when the properties of the soil increase with depth?

To gain insight in radiation damping of unbounded soil (Wolf and Song 1996, Sections 5.2.11 and 5.2.12), it is assumed that the shear modulus and mass density vary as

$$G(r) = G_0 \left(\frac{r}{r_0}\right)^g \qquad (1a) \qquad\qquad \rho(r) = \rho_0 \left(\frac{r}{r_0}\right)^m \qquad (1b)$$

where r is the radial coordinate measured from the centre O towards infinity (Figure 1). G_0 and ρ_0 are the values at the structure-soil interface with r_0. The powers g and m are real numbers, which can be selected as positive or negative. The shear-wave velocity is written as

$$c_s(r) = \sqrt{\frac{G(r)}{\rho(r)}} = c_{s0} \left(\frac{r}{r_0}\right)^{\frac{g}{2}-\frac{m}{2}} \qquad (2a) \qquad \text{with} \qquad c_{s0} = \sqrt{\frac{G_0}{\rho_0}} \qquad (2b)$$

[1] *Institute of Hydraulics and Energy, Civil Eng, Swiss Federal Institute of Tech, Lasanne, Switzerland. john.wolf@epfl.ch*
[2] *Passera & Pedretti Consulting Engineers, Via al Molino 6, CH-6916 Grancia, Switzerland*

In the derivation of the radiation criterion, another fictitious interface with radial coordinate r (dashed line in Figure 1), which is similar to the structure-soil interface with r_0, is introduced. Between these two interfaces a finite-element cell is created. By repeating this procedure the unbounded soil can be represented by infinitely many similar finite-element cells (infinite substructuring). When in the limit $r \to \infty$ the *inertial force* of the cell dominates over the *elastic restoring force*, energy is propagated and radiation damping exists. This is satisfied for

$$1 - \frac{g}{2} + \frac{m}{2} > 0 \qquad (3a) \qquad \text{or} \qquad c_s(r) < c_{s0}\frac{r}{r_0} \qquad (3b)$$

for all frequencies ω. When the elastic restoring force dominates over the inertial force, no energy is propagated and radiation damping vanishes. This applies for

$$1 - \frac{g}{2} + \frac{m}{2} < 0 \qquad (4a) \qquad \text{or} \qquad c_s(r) > c_{s0}\frac{r}{r_0} \qquad (4b)$$

for all ω. In the intermediate case

$$1 - \frac{g}{2} + \frac{m}{2} = 0 \qquad (5a) \qquad \text{or} \qquad c_s(r) = c_{s0}\frac{r}{r_0} \qquad (5b)$$

the elastic restoring force and the inertial force dominate for sufficiently small and large frequencies, respectively. Thus, a *cutoff frequency* exists below which no radiation damping exists. Equations 3, 4 and 5 describe the *radiation criterion*. For instance, it follows from equation 4, that no radiation damping will occur in an unbounded soil when the shear modulus increases sufficiently in the radial direction.

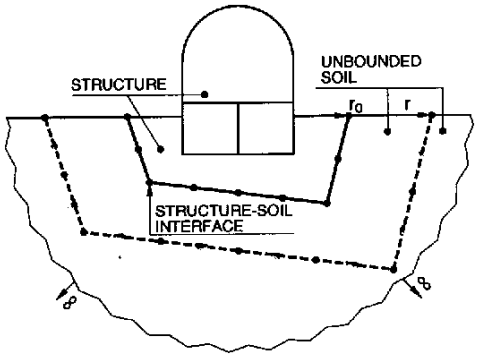

Figure 1. Problem definition of dynamic soil-structure interaction

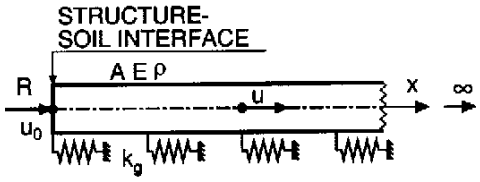

Figure 2. Semi-infinite rod on elastic foundation

2 RADIATION CONDITION REFERS TO ENERGY NOT WAVES

The radiation condition (Sommerfeld 1948) states that no *energy* may be radiated from infinity into the soil towards the source. This does not necessarily mean that outwardly propagating waves are present, as is clearly demonstrated in Schill (1988).

The semi-infinite rod with area A, modulus of elasticity E, hysteretic damping ratio ζ and mass density ρ on an elastic foundation with static stiffness per unit length k_g (Figure 2) represents the unbounded soil. The equation of motion in the displacement amplitude $u(\omega)$ is straightforwardly formulated (Wolf and Song 1996, Section A.2) with $u = u(\omega)e^{+i\omega t}$ as

$$E(1+2i\zeta)u(\omega)_{,xx} - \frac{k_g}{A}u(\omega) + \omega^2\rho u(\omega) = 0 \qquad (6)$$

For $\zeta \ll 1$ the solution equals

$$u(\omega) = c_1 e^{+\omega\zeta\frac{x}{c(\omega)}} e^{+i\omega\frac{x}{c(\omega)}} + c_2 e^{-\omega\zeta\frac{x}{c(\omega)}} e^{-i\omega\frac{x}{c(\omega)}} \qquad (7a) \qquad u(\omega) = c_1 e^{-\omega\frac{x}{d(\omega)}} e^{+i\omega\zeta\frac{x}{d(\omega)}} + c_2 e^{+\omega\frac{x}{d(\omega)}} e^{-i\omega\zeta\frac{x}{d(\omega)}} \qquad (7b)$$

with the phase velocities

$$c(\omega) = \sqrt{\frac{E}{\rho}} \frac{1}{\sqrt{1 - \frac{1}{\omega^2}\frac{k_g}{A\rho}}} \qquad (8a) \qquad \text{and} \qquad d(\omega) = \sqrt{\frac{E}{\rho}} \frac{1}{\sqrt{\frac{1}{\omega^2}\frac{k_g}{A\rho} - 1}} \qquad (8b)$$

Equations 7a and 7b are interpreted for $\omega > \omega_c$ and $\omega < \omega_c$, respectively, with the cutoff frequency $\omega_c = \sqrt{k_g/(A\rho)}$. The integration constants c_1 and c_2 are determined for the two cases addressing the amplitudes at infinity. For $\omega > \omega_c$, the amplitude of the first term in Equation 7a tends to infinity for $x \to \infty$, leading to $c_1 = 0$. The remaining term with c_2 corresponds to wave propagation in the positive $x-$ direction $e^{+i\omega(t-x/c(\omega))}$, i.e. outwardly propagating waves, with an exponentially decreasing amplitude for $x \to \infty$. This behaviour is to be expected. For $\omega < \omega_c$, the amplitude of the second term in equation 7b tends to infinity for $x \to \infty$, leading to $c_2 = 0$. The remaining physically acceptable term with c_1 corresponds to wave propagation in the negative $x-$ direction $e^{+i\omega(t+x/d(\omega))}$, i.e. *incoming waves*, again with an exponentially decreasing amplitude for $x \to \infty$. This behaviour is surprising.

For this latter case, the radiation of energy at infinity is addressed. For radiation of energy towards infinity, i.e. in the positive $x-$ direction to occur, the imaginary part of the dynamic-stiffness coefficient must be positive (energy is dissipated, not created). The dynamic-stiffness coefficient $S(\omega)$ determined e.g. at $x = 0$ relates the amplitude of the displacement $u_0(\omega)$ to that of the interaction force $R(\omega)$ (Figure 2)

$$R(\omega) = S(\omega)u_0(\omega) \qquad (9)$$

Substituting equation 7b with $c_2 = 0$ in

$$R(\omega) = -EAu_{0,x}(x) \qquad (10)$$

yields

$$S(\omega) = \sqrt{EAk_g}\sqrt{1 - \omega^2\frac{A\rho}{k_g}}(1 + i\zeta) \qquad (11)$$

For the case with incoming waves ($\omega < \omega_c$) it follows that the imaginary part is positive (The same also applies for the other case $\omega > \omega_c$).

Summarizing, for the damped semi-infinite rod on elastic foundation, the *radiation condition* expressing that energy is radiated towards infinity *corresponds to* outwardly propagating waves for $\omega > \omega_c$, but to *incoming waves* for $\omega < \omega_c$. The direction of the transmission of energy is thus opposite to that of the phase velocity for this latter case. (The amplitude decays towards infinity in both cases). The significance of this example is much greater than expected, as it also represents exactly a singlemode of an infinite modal expansion of the out-of-plane response of a soil layer fixed on rigid rock.

3 DIMENSIONLESS FREQUENCY

It is well known that the *dynamic stiffness* of the unbounded soil *is a function of the dimensionless frequency*, which is proportional to the product of the frequency ω and the radial coordinate r (characteristic length of the structure-soil interface), but not explicitly e.g. of ω. In Figure 1 the radial coordinate of the structure-soil interface, measured from the appropriately chosen centre O, equals r_0. It is permissible to select another in this case similar structure-soil interface further away from the structure with the radial coordinate r (dashed line). The region between the two interfaces is regarded as part of the structure. In this case the dimensionless frequency associated with the dynamic stiffness will increase. For larger dimensionless frequencies the dynamic stiffness of the unbounded soil is smoother. This can be illustrated addressing the dimensionless high-frequency expansion of the dynamic-stiffness matrix (Song and Wolf 1998)

$$[S(\omega, r)] = \left(\frac{r}{r_0}\right)^{s-2}\left(i\omega\frac{r}{r_0}[C_\infty] + [K_\infty] + \sum_{j=1}^{m}\left(i\omega\frac{r}{r_0}\right)^{-j}[A_j]\right) \qquad (12)$$

where $[C_\infty]$, $[K_\infty]$, $[A_j]$ are constants and s denotes the spatial dimension ($= 2$ or $= 3$). The smoothness of $[S]$ for large ωr makes the modelling easier, permitting approximate local transmitting boundaries to be used. For an unbounded soil layer on rigid rock (Figure 3), the radial coordinate of the structure-soil interface is constant (centre O at infinity). Thus placing the structure-soil interface further away (dashed line) does not help! This is verified addressing the dynamic-stiffness coefficient in node 1, corresponding to a parabolic out-of-plane motion on the vertical structure-soil interface (Figure 4), of an unbounded soil layer of depth d on rigid rock (Wolf 1998, Section 3.9.3). The real and imaginary parts of the exact solution are shown as solid and dotted lines, respectively (Figure 5).

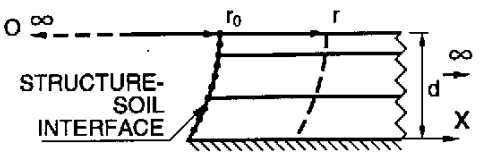

Figure 3. Horizontally stratified soil layer on rigid rock

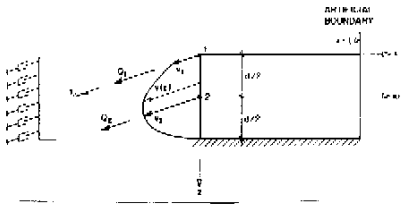

Figure 4. Out-of-plane motion of soil layer on rigid rock

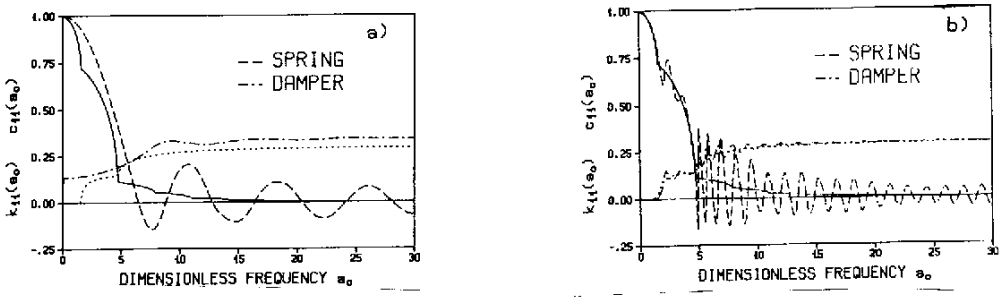

Figure 5. Dynamic-stiffness coefficient for viscous boundary. a. $l/d = 0.4$. b. $l/d = 2$

$$S_{11}(a_0) = K[k_{11}(a_0) + ia_0c_{11}(a_0)] \tag{13}$$

with $a_0 = \omega d/c_s$ (shear-wave velocity c_s). K represents the static-stiffness coefficient. Shifting the interface where the dynamic behaviour of the remaining unbounded soil up to infinity is modelled approximately with viscous dashpots by the distance l denoted as artificial boundary leads for harmonic excitation to errors which do not depend on l/d (Figure 5 with results for two ratios). In general, for efficiency, the (global) interaction force-displacement relationship of the unbounded soil should be formulated on the structure-soil interface.

4 SIMPLE PHYSICAL MODELS

Just as engineering beam theory in stress analysis is based on assumed displacement patterns instead of rigorous elasticity solutions, the simple physical models present a major step towards developing *a strength-of-materials approach to foundation dynamics* (Wolf 1994). The physical models consist of the following representations (Figure 6)

1. *Cones.* Translational and rotational truncated semi-infinite cones are based on rod (bar) theory (plane sections remain plane) with the corresponding one-dimensional displacement.
2. *Spring-Dashpot-Mass Models* with frequency-independent coefficients and a few internal variables. The unbounded soil is represented by the same type of dynamic model as the structure, enabling the same structural dynamics program to be applied.
3. *Prescribed wave patterns in the horizontal plane.* These are one-dimensional body and surface waves on the free surface and cylindrical waves.

The described procedures satisfy the following requirements: *Conceptual clarity and physical insight. Simplicity in physical description* (e.g., one-dimensional, not three-dimensional wave propagation) *and in application*, permitting an analysis with a hand calculator in many cases. *Sufficient scope of application* (shape of foundation, soil profile, embedment, piles). *Sufficient engineering accuracy.* The advantages lead to the direct use in engineering practice for everyday design of machine foundations and structures founded on soil subjected to dynamic loads (dynamic soil-structure interaction) such as earthquakes, explosions, waves, traffic excitation, and so on. Possibility to check the results of more sophisticated analyses.

As an extension, the simple dynamic Green's function (Wolf 1994 Chapter 5) can be used to calculate the vertical displacement w on the free surface of a half-space (Figure 7) due to a vertical concentrated load travelling horizontally with the velocity v (Duvernay 1995). Two subsonic cases ($v <$ shear-wave velocity) with Poisson's ratio = 0.25 are presented. For $v <$ Rayleigh-wave velocity v_R ($v/v_R = 0.99$) the (dimensionless) displacement (Figure 8) is symmetric fare and aft, i.e. with respect to the line $\theta = 90°$ (shear modulus G). The exact solution is specified in Lansing 1966. For $v > v_R$ ($v/v_R = 1.04$), i.e. when the load outruns the Rayleigh wave, the distribution of w changes abruptly (Figure 9). An infinite discontinuity occurs and the direction is reversed. Good agreement

with the exact solution is again achieved. The transonic and supersonic cases perform equally well (results not shown).

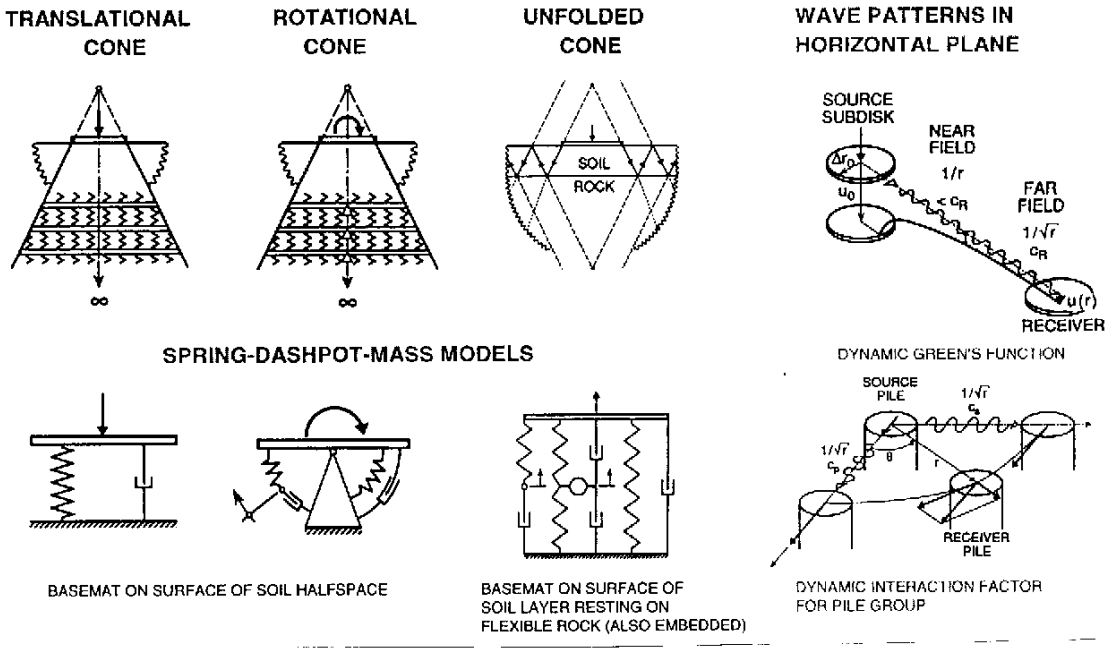

Figure 6. Simple physical models to represent the unbounded soil

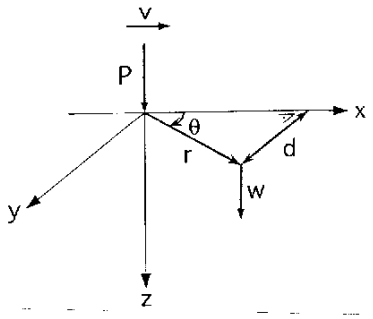

Figure 7. Vertical concentrated load moving over the surface of a half-space

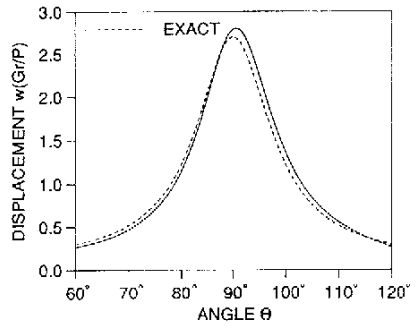

Figure 8. Vertical displacement for velocity of load lower than Rayleigh-wave velocity

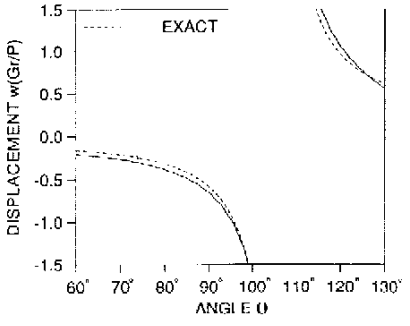

Figure 9. Vertical displacement for velocity of load higher than Rayleigh-wave velocity

5 DAMPING-SOLVENT EXTRACTION METHOD

The unbounded soil is modelled based on finite-element concepts only (Wolf and Song 1996, Part II). A finite region of the unbounded soil adjacent to the structure is modelled with finite elements. *Damping*, which is not

present in the actual soil, *is introduced artificially* to reduce the amplitudes of outwardly propagating waves and waves reflected from the outer boundary. This results in a dynamic-stiffness matrix for the structure-soil interface which depends upon outwardly propagating waves only. This matrix is then assumed to represent the unbounded soil with the same artificial damping. Finally, the influence of the introduced artificial damping is *extracted*, whereby this very simple operation can be performed for each element of the matrix and for each frequency independently from the others. The damping-solvent extraction method can also be applied directly in the time domain.

6 SCALED BOUNDARY FINITE-ELEMENT METHOD

6.1 Concept

In this *semi-analytical boundary-element method based on finite elements* only the structure-soil interface is discretized with surface finite elements yielding a reduction of the spatial dimension by one. No fundamental solution is necessary and thus no singular integrals must be evaluated and general anisotropic material can be analysed. The *radiation condition* at infinity *is satisfied exactly*. No discretization of free and fixed boundaries such as the free surface and interfaces between different materials is required. Thus, the scaled boundary finite-element method (Wolf and Song 1996, Part I, Song and Wolf 1997) not only combines the advantages of the finite-element and boundary-element methods but also presents appealing features of its own.

A coordinate transformation from the Cartesian coordinate system $\hat{x}, \hat{y}, \hat{z}$ to the system with the dimensionless radial coordinate ξ ($1 \leq \xi < \infty$ for the unbounded soil) and the circumferential coordinates η, ζ on each finite element on the structure-soil interface is performed (Figure 10). After applying a weighted-residual formulation in the circumferential directions, the governing partial differential equations of linear elastodynamics are transformed to the scaled boundary finite-element equation in displacement, a system of linear second-order ordinary differential equations with the radial coordinate ξ as independent variable

$$[E^0]\xi^2\{u(\xi)\}_{,\xi\xi} + ((s-1)[E^0] - [E^1] + [E^1]^T)\xi\{u(\xi)\}_{,\xi} + ((s-2)[E^1]^T - [E^2])\{u(\xi)\} + \omega^2[M^0]\xi^2\{u(\xi)\} = 0 \quad (14)$$

$\{u(\xi)\}$ are the displacement amplitudes at ξ corresponding to the degrees of freedom in the nodes on the structure-soil interface, and s is the spatial dimension ($= 2$ or $= 3$). The coefficient matrices $[E^0]$, $[E^1]$, $[E^2]$ and $[M^0]$ are calculated and assembled similarly as the static-stiffness and mass matrices of finite elements on the structure-soil interface. Equation 14 can be solved analytically (Song and Wolf 1998). The scaled boundary finite-element method is analytical in the radial direction and numerical in the finite-element sense in the circumferential directions parallel to the boundary.

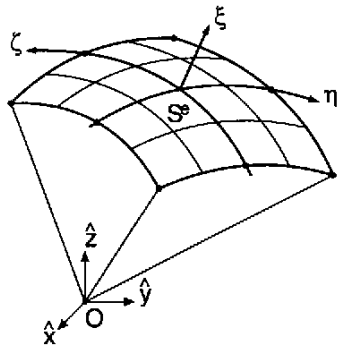

Figure 10. Scaled boundary transformation of geometry of surface finite element on structure-soil interface

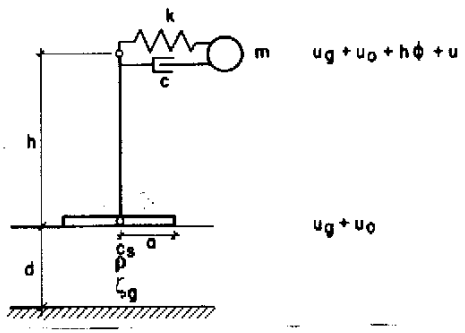

Figure 11. Coupled dynamic model of structure and soil with 3 degrees of freedom

6.2 Reduced Set of Base Functions

To increase the computational efficency of the scaled boundary finte-element method, the displacement amplitudes $\{u(\xi)\}$ in equation 14 are represented with a reduced set of base functions $[\Phi]$ and corresponding amplitudes

$\{v(\xi)\}$

$$\{u(\xi)\} = [\Phi]\{v(\xi)\} \tag{15}$$

Equation 14 is transformed to

$$[e^0]\xi^2\{v(\xi)\}_{,\xi\xi} + ((s-1)[e^0] - [e^1] + [e^1]^T)\xi\{v(\xi)\}_{,\xi} + ((s-2)[e^1]^T - [e^2])\{v(\xi)\} + \omega^2[m^0]\xi^2\{v(\xi)\} = 0 \tag{16}$$

with the coefficent matrices

$$[e^0] = [\Phi]^T[E^0][\Phi] \quad \ldots \quad (17a) \qquad [m^0] = [\Phi]^T[M^0][\Phi] \tag{17b}$$

As the dynamic stiffness at low frequency dominates, in general, the dynamic response in soil-structure interaction, the reduced set of base functions $[\Phi]$ is selected from the solution of equation 14 for statics. The first few eigenfunctions determine $[\Phi]$.

7 MODEL WITH FINITE NUMBER OF DEGREES OF FREEDOM FOR UNBOUNDED SOIL

The interaction force-displacement relationship involves a convolution integral of the unit-impulse response and the displacement. This integral has to be recalculated from time zero onwards for each time station in an analysis of a transient. In this rigorous evaluation of the convolution integrals a larger computational effort (proportional to the *square* of the number of time stations) and storage requirement result, which makes it unrealistic to perform large practical (nonlinear) unbounded soil-structure-interaction analyses with many degrees of freedom on the structure-soil interface.

To reduce the computational effort the concepts of *linear system theory* can be applied. The methods approximate the dynamic stiffness by a rational function in $i\omega$, corresponding to a *dynamic system with a finite number of degrees of freedom* (Paronesso 1997, Wolf and Song 1996, Section 2.4). This results in a reduced computational effort (proportional to the number of time stations) and storage requirement, as in the dynamic analysis of a structure.

8 EQUIVALENT ONE-DEGREE-OF-FREEDOM SYSTEM

To study the response of a single-degree-of-freedom structure (structural distortion u) with stiffness k, mass m, height h and base radius a including the interaction with the soil (in addition horizontal base displacement u_0 and rotation ϕ) (shear-wave velocity c_s, mass density ρ) to a horizontal earthquake motion u_g (Figure 11), an equivalent one-degree-of-freedom system can be constructed (Wolf 1985, Section 9.1, Wolf 1994, Section 7.2). Its equivalent natural frequency $\tilde{\omega}$ and damping ratio $\tilde{\zeta}$ follow from the following simple equations

$$\frac{1}{\tilde{\omega}^2} = \frac{1}{\omega_s^2} + \frac{1}{\omega_h^2(\tilde{a}_0)} + \frac{1}{\omega_r^2(\tilde{a}_0)} \tag{18}$$

with the fixed-base frequency of the structure $\omega_s = \sqrt{k/m}$ and the horizontal and rocking soil frequencies for a rigid structure

$$\omega_h(a_0) = \sqrt{\frac{K_h k_h(a_0)}{m}} \quad (19a) \qquad \omega_r(a_0) = \sqrt{\frac{K_r k_r(a_0)}{mh^2}} \tag{19b}$$

where the horizontal and rocking dynamic-stiffness coefficients of the soil equal

$$S_h(a_0) = K_h k_h(a_0)(1 + 2i\zeta_h(a_0) + 2i\zeta_g) \quad (20a) \qquad S_r(a_0) = K_r k_r(a_0)(1 + 2i\zeta_r(a_0) + 2i\zeta_g) \tag{20b}$$

with the radiation-damping ratios of the undamped soil

$$\zeta_h(a_0) = \frac{a_0 c_h(a_0)}{2k_h(a_0)} \quad (21a) \qquad \zeta_r(a_0) = \frac{a_0 c_r(a_0)}{2k_r(a_0)} \tag{21b}$$

The dynamic-stiffness coefficients of the undamped soil are defined as

$$S_h(a_0) = K_h(k_h(a_0) + 2ia_0 c_h(a_0)) \quad (22a) \qquad S_r(a_0) = K_r(k_r(a_0) + 2ia_0 c_r(a_0)) \tag{22b}$$

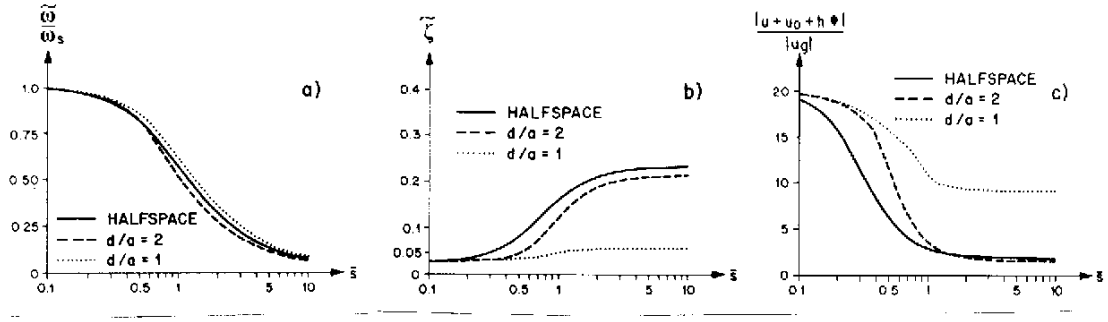

Figure 12. Equivalent properties and harmonic response ($h/a = 0.67$, $m/(\rho a^3) = 3$, $\nu = 0.33$, $\zeta = 0.025$, $\zeta_g = 0.05$) varying depth of layer. (a) Natural frequency; (b) damping; (c) displacement of mass relative to free field motion u_g

with the dimensionless frequency $a_0 = \omega a/c_s$ and $\tilde{a}_0 = \tilde{\omega} a/c_s$. K_h and K_r are the static-stiffness coefficients. ζ_g is the hysteretic material damping ratio of the soil.

$$\tilde{\zeta} = \frac{\tilde{\omega}^2}{\omega_s^2}\zeta + \left(1 - \frac{\tilde{\omega}^2}{\omega_s^2}\right)\zeta_g + \frac{\tilde{\omega}^2}{\omega_h^2(\tilde{a}_0)}\zeta_h(\tilde{a}_0) + \frac{\tilde{\omega}^2}{\omega_r^2(\tilde{a}_0)}\zeta_r(\tilde{a}_0) \tag{23}$$

with the hysteretic damping ratio ζ of the structure. $\tilde{\zeta}$ is equal to the sum of the contributions of the four damping mechanisms.

The equivalent one-degree-of-freedom system, possibly defined slightly differently, has been used extensively to analyse interaction effects when the soil is modelled as a homogeneous half-space. It can, however, just as well be used to address a soil layer of depth d resting on rigid rock (Figure 11). Physical insight can be gained. For the dimensionless parameters specified in the caption of Figure 12 $\tilde{\omega}/\omega_s$ and $\tilde{\zeta}$ are plotted as a function of the stiffness ratio $\bar{s} = \omega_s h/c_s$ in Figures 12a and 12b. For increasing $\bar{s}$ $\tilde{\omega}/\omega_s$ decreases from 1, hardly being effected by the site. $\tilde{\zeta}$ increases significantly for the half-space, mostly due to radiation damping. For the shallow soil layer $d/a = 1$ no radiation damping is activated, as $\tilde{\omega}$ lies for all $\bar{s}$ below the cutoff frequency of the soil layer, which is equal to the fundamental frequency of the soil layer. $\tilde{\zeta}$ starts at $\zeta = 0.025$ and tends towards $\zeta_g = 0.05$ (equation 23). The amplitude of the maximum displacement of the mass relative to the free-field motion (determined at $\omega = \tilde{\omega}$) is plotted in Figure 12c. The effect of the smaller $\tilde{\zeta}$ of the layer with $d/a = 1$ leading to a larger response compared to that of the half-space is clearly visible.

REFERENCES

Duvernay, B. (1995). "Personal communication". *(Internal Report).*

Lansing, D. L. (1966). "The displacements in an elastic half-space due to a moving concentrated normal load". *NASA Technical Report* NASA TR R-238.

Paronesso, A. (1997). *Rational Approximation and Realization of Generalized Force-Displacement Relationship of an Unbounded Medium.* Ph.D-thesis No 1611, Swiss Federal Institute of Technology Lausanne.

Schill, M. (1988). "A critical study of the "radiation condition" for longitudinal waves in a damped semi-infinite bar supported by an ambient medium". *Journal of Sound and Vibration* **125**(1), 131–135.

Sommerfeld, A. (1949). *Partial Differential Equations in Physics*, Chapter 28. Academic Press, New York.

Song, C. and Wolf, J. P. (1997). "The scaled boundary finite-element method – alias consistent infinitesimal finite-element cell method – for elastodynamics". *Computer Methods in Applied Mechanics and Engineering* **147**, 329–355.

Song, C. and Wolf, J. P. (1998). "The scaled boundary finite-element method: analytical solution in frequency domain". *Computer Methods in Applied Mechanics and Engineering* **164**, 249–264.

Wolf, J. P. (1985). *Dynamic Soil-Structure Interaction*. Prentice-Hall, Englewood Cliffs.

Wolf, J. P. (1988). *Soil-Structure-Interaction Analysis in Time Domain*. Prentice-Hall, Englewood Cliffs.

Wolf, J. P. (1994). *Foundation Vibration Analysis Using Simple Physical Models*. Prentice-Hall, Englewood Cliffs.

Wolf, J. P. and Song, C. (1996). *Finite-Element Modelling of Unbounded Media*. John Wiley & Sons, Chichester.